Measurement of Contact-Angle Hysteresis for Droplets on Nanopillared Surface and in the Cassie and Wenzel States: A Molecular Dynamics Simulation Study

Takahiro Koishi,[†,*] Kenji Yasuoka,[‡] Shigenori Fujikawa,[¶,⊥] and Xiao Cheng Zeng[§,*]

[†]Department of Applied Physics, University of Fukui, 3-9-1 Bunkyo, Fukui 910-8507, Japan, [‡]Department of Mechanical Engineering, Keio University, Yokohama 223-8522, Japan, [¶]Interfacial Nanostructure Research Laboratory, RIKEN, Wako, Saitama, 351-0198, Japan, [§]Department of Chemistry, University of Nebraska, Lincoln, Nebraska 68588, United States, and [⊥]JST, CREST, Wako, Saitama, 351-0198, Japan

ABSTRACT We perform large-scale molecular dynamics simulations to measure the contact-angle hysteresis for a nanodroplet of water placed on a nanopillared surface. The water droplet can be in either the Cassie state (droplet being on top of the nanopillared surface) or the Wenzel state (droplet being in contact with the bottom of nanopillar grooves). To measure the contact-angle hysteresis in a quantitative fashion, the molecular dynamics simulation is designed such that the number of water molecules in the droplets can be systematically varied, but the number of base nanopillars that are in direct contact with the droplets is fixed. We find that the contact-angle hysteresis for the droplet in the Cassie state is weaker than that in the Wenzel state. This conclusion is consistent with the experimental observation. We also test a different definition of the contact-angle hysteresis, which can be extended to estimate hysteresis between the Cassie and Wenzel state. The idea is motivated from the appearance of the hysteresis loop typically seen in computer simulation of the first-order phase transition, which stems from the metastability of a system in different thermodynamic states. Since the initial shape of the droplet can be controlled arbitrarily in the computer simulation, the number of base nanopillars that are in contact with the droplet can be controlled as well. We show that the measured contact-angle hysteresis according to the second definition is indeed very sensitive to the initial shape of the droplet. Nevertheless, the contact-angle hystereses measured based on the conventional and new definition seem converging in the large droplet limit.

KEYWORDS: contact angle · hysteresis · Wenzel and Cassie states · nanopillared surface · molecular dynamics simulation

The contact angle for a liquid droplet on a surface is commonly used to characterize wettability of the surface. However, if molecules are added or removed from the liquid droplet, the droplet can spread or retract on the surface, and as such, the apparent contact angle is generally different from the equilibrium contact angle. When the extraction of maximum liquid volumes from the droplet is achieved without reducing the contact area, the receding contact angle is measured. When the addition of maximum volumes to the droplet is achieved without increasing the contact area, the advancing contact angle is measured. The difference between the advancing contact angle and the receding contact angle is defined as the contact-angle hysteresis. This conventional definition of the contact-angle hysteresis (hereafter we call it definition I) is widely used in experiments. To our knowledge, the earliest measurement of the contact-angle hysteresis was reported by Johnson and Dettre in 1964.[1] They measured the contact-angle hysteresis for water droplets on rough hydrophobic surfaces.

It is known that the measured contact-angle hysteresis can be strongly dependent on the state of the droplet especially if the surface is rough. Typically, on a rough hydrophobic surface, water droplets can be either in the Wenzel state[2] (for which the water droplets are in full contact with the surface grooves) or in the Cassie state[3] (for which the water droplets are in contact with only the tips of the surface structures, while "air pockets" can be trapped between grooves of the surface structure[4]). Hence, if a surface is engineered such that the droplet can exhibit both Cassie and Wenzel states (*i.e.*, bistability) on the surface, the measurement of contact-angle hysteresis can be tricky because the measured hysteresis would depend on whether the droplet is in the Cassie or in the Wenzel state or whether or not a transition from Cassie to Wenzel state would occur during the measurement. Patanker and coworkers conducted such a measurement on well-designed micropillared surfaces.[5] They

* Address correspondence to koishi@u-fukui.ac.jp, xzeng1@unl.edu.

Received for review February 10, 2011 and accepted August 13, 2011.

Published online August 14, 2011
10.1021/nn2005393

showed that the advancing contact angle and the receding contact angle of the droplets were different in the Cassie state when the aspect ratio of the micropillars was very large. They observed that when a droplet was placed gently on the surface, the contact angle was larger than that when it was dropped from some height. Their results indicate that the measured contact angle can be dependent on how the droplet is placed on the surface.

Lafuma and Quéré[6] also measured the contact-angle hysteresis for water droplets (in the Wenzel or Cassie state) on a microtextured surface. They reported that the contact angle of a water droplet was 164° and the contact-angle hysteresis was 5°, which was very small. They found that there were air pockets between the droplet and the textured surface so that the droplet was in the Cassie state. They also measured the contact angle of a droplet in the Wenzel state (obtained by condensing water vapor). The contact angle was 141°, and the contact-angle hysteresis was 100−105° . They concluded that the contact-angle hysteresis in the Cassie state was much weaker than that in the Wenzel state. In addition, they demonstrated that a direct transition from the Cassie state to the Wenzel state can be induced by applying a pressure, and this transition was irreversible. Reyssat and Quéré[7] measured the contact-angle hysteresis in the Cassie state on designed pillared surfaces. They found that the contact-angle hysteresis became larger with increasing the pillar density, and the hysteresis was independent of the droplet volume. Meanwhile, they calculated the contact-angle hysteresis theoretically as a function of the pillar density. The agreement between the experimental measurement and theoretical calculation was good except for regions of low and high pillar densities. Extrand[8] suggested that droplet conditions on a rough surface depended on the contact line density. The latter is defined as the length of the pillar perimeter (per unit area) that can potentially suspend a droplet. This density can be used to predict whether the droplet favors the Wenzel state or the Cassie state and the magnitude of the contact-angle hysteresis. Recently, Liu *et al*. demonstrated that certain superhydrophobic surfaces can lose their water repellency when the water is hot, and this change of wetting state of water droplets was attributed to the transition from the Cassie state to the Wenzel state.[9]

Several computer simulations and theoretical calculations were performed to understand the contact-angle hysteresis phenomena.[10−14] Hong *et al*.[13] computed the contact angle of moving droplets by means of molecular dynamics (MD) simulation. They applied a body force to move droplets on three different solid surfaces; each entailed different interaction with water. Their results showed that the contact-angle hysteresis became larger with increasing the strength of attractive force between the surface and water molecules.

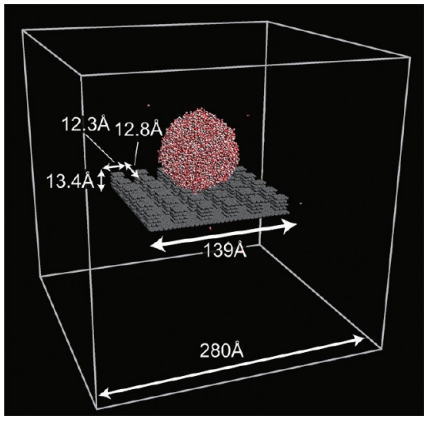

Figure 1. Schematic plot of the simulation system.

Recently we reported results of two independent MD simulations of water[15] and urea−water droplets[16] on nanopillared surfaces. We observed the coexistence of the Wenzel and Cassie states and estimated the height of the free energy barrier separating the Wenzel and Cassie states. In this article, we report, to our knowledge, the first systematic simulation study of the contact-angle hysteresis for water droplets on a nanopillared surface. To compute the contact angles and contact-angle hysteresis, we have devised a series of MD simulations of water droplets with different sizes. In addition, we have tested a different computational approach to characterize the contact-angle hysteresis, namely, initial-condition-dependent contact-angle hysteresis. This definition is for computer simulation only, which is motivated from the behavior of the hysteresis loop typically seen in computer simulation of the first-order phase transition, owing to metastability of a system in different states.

SIMULATION RESULTS

The simulation supercell contains a water droplet and a nanopillared surface (Figure 1). The surface is the (0001) graphite surface with hexagonally arranged carbon atoms. During the simulation carbon atoms are fixed. The nanopillared surface consists of an ordered array of quadrangular nanopillars whose lateral size is 12.3 Å × 12.8 Å. The spatial interval between the nanopillars is 12.3 Å and 12.8 Å in the *x* and *y* direction, respectively. This near-square-lattice arrangement for the nanopillar array has been used previously by Lundgren *et al*.[21,22] The height of the nanopillars is 13.4 Å, equivalent to the height of four stacked graphene layers. The lateral length scale of the nanopillared array is 139 Å, and the supercell contains 6 × 6 nanopillars. By gradually changing the number of water molecules in the droplet, we can study the effect of adding or reducing the volume of a droplet, as in the experimental measurement of the contact-angle hysteresis.

First, we examine droplet size dependence of the contact angle on a flat surface in order to detect the

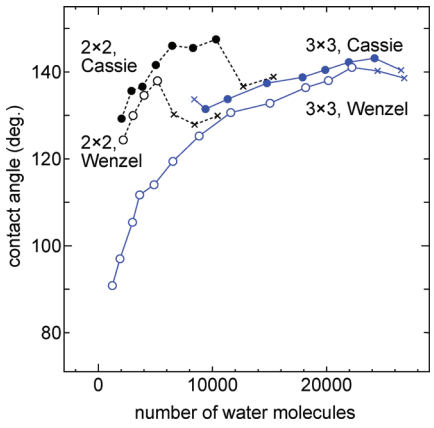

Figure 2. Droplet size dependence of the computed contact angles for a droplet in four initial conditions: in contact with 2 × 2 base nanopillars and in the Cassie state (filled circles with dotted line); in contact with 2 × 2 base nanopillars and in the Wenzel state (open circles with dotted line); in contact with 3 × 3 base nanopillars and in the Cassie state (filled circles with solid line); and in contact with 3 × 3 base nanopillars and in the Wenzel state (filled circles with solid line). The crosses indicate that the size of the droplet becomes too small or too large to be supported by the initially assigned base nanopillars.

line tension effect on the apparent contact angle. This effect has been studied by several groups using MD or Monte Carlo (MC) simulations.[17−20] The line tension can be computed from the size dependence of the contact angle.[17] We compute the contact angle of a droplet in the size range N = 12 000−100 000 on the flat surface (see Simulation Method). In this size range, the variation in the contact angle is less than 1°. Hence, we conclude that the line tension effect is very small for our system.

In all subsequent simulations, the numbers of base nanopillars in contact with the droplet are either 2 × 2, 3 × 3, or 4 × 4. Initially, the droplet can be either in the Wenzel or in the Cassie state. To record the number of base nanopillars that are in direct contact with the droplet during the simulation, we identify those carbon atoms that are in close contact to water molecules. At an instant, any carbon atom that has two or more water molecules located within 5.26 Å distance from it is referred to as the contact carbon atom. The reason for choosing at least two water molecules is to avoid counting the collision between a water molecule (in the vapor) with a carbon atom as a contact. The value of 5.26 Å corresponds to the first minimum of the radial distribution function of carbon−water.

Figure 2 shows the calculated contact angle as a function of the size of a droplet in four different initial conditions: the droplet is (1) in contact with 2 × 2 base nanopillars and in the Cassie state; (2) in contact with 2 × 2 base nanopillars and in the Wenzel state; (3) in contact with 3 × 3 base nanopillars and in the Cassie state; and (4) in contact with 3 × 3 base nanopillars and in the Wenzel state. The crosses in Figure 2 indicate that the size of the droplet becomes too small or too large to be supported by the initial number of base nanopillars. For most of these states marked by the crosses, the number of base nanopillars in contact with the droplet increases during the simulation, indicating that the contact angle decreases.

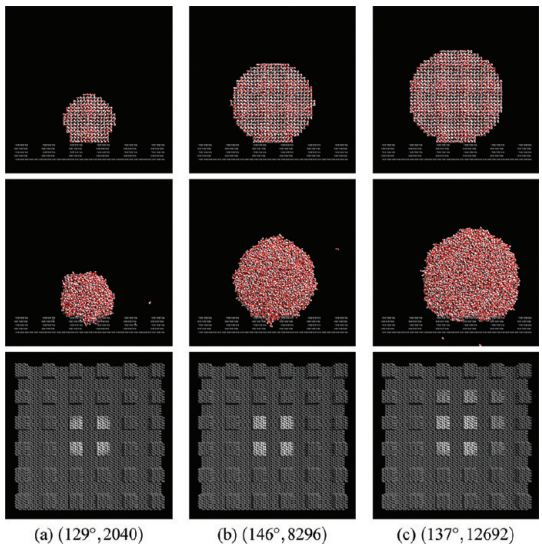

Figure 3. Initial configurations (top panel), snapshots of droplets at t = 1.0 ns (middle panel), and the carbon atoms in contact with the droplet (bottom panel, highlighted by white color) on the 2 × 2 base nanopillars and in the Cassie state. The measured contact angle and the number of water molecules are (a) (129°, 2040), (b) (146°, 8296), and (c) (137°, 12 692).

Figure 3 shows the initial configuration of water droplets, snapshots of the droplets at t = 1.0 ns, and carbon atoms directly in contact with water. All the simulations start from the same initial condition for the droplet; that is, the droplet is located on the 2 × 2 base nanopillars and in the Cassie state (see top panel in Figure 3). In Figure 3, we also display snapshots of those carbon atoms in direct contact with water. Here, we use the degree of brightness for carbon atoms to illustrate the probability of being in contact with water during the 1.0 ns simulations. The white-colored carbon atoms indicate that they are always in contact with the water molecules during the simulation. As shown in Figure 3a and b, the number of base nanopillars supporting the droplet is unchanged for smaller droplets. In this case, the contact angle of the droplets increases with increasing the number of water molecules (*i.e.*, effect of adding volume of water) as the bottom of the droplets is pinned by the edges of the base nanopillars. With the 2 × 2 base nanopillars, the maximum number of water molecules supported is about N = 10 000, as shown in Figure 2. When the size of the droplet is greater than this size, the droplet starts to make contact with nanopillars beyond the initial base nanopillars and the contact angle starts to decrease, as shown in Figure 3c and Supporting Information (SI) Movie S1. To estimate the error bar for the maximum number of water molecules shown in

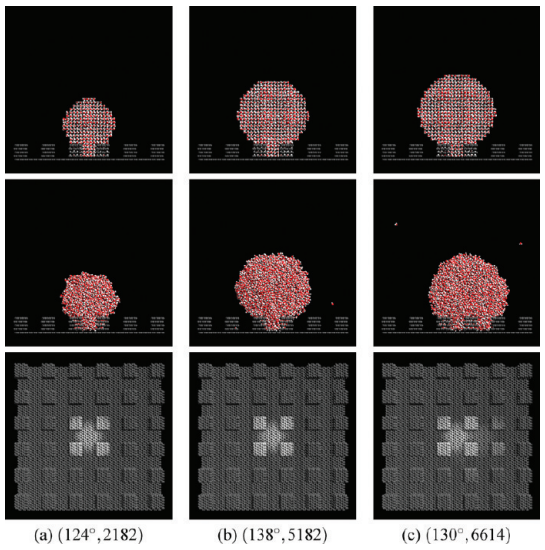

Figure 4. Initial configurations (top panel), snapshots of droplets at $t = 1.0$ ns (middle panel), and the carbon atoms in contact with the droplet (bottom panel, highlighted by white color) on the 2 × 2 base nanopillars in the Wenzel state. The measured contact angle and the number of water molecules are (a) (124°, 2182) (left column), (b) (138°, 5182) (middle column), and (c) (130°, 6614) (right column).

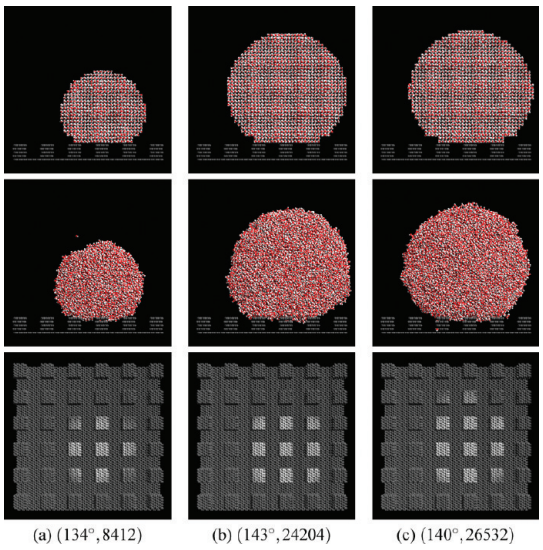

Figure 5. Initial configurations (top panel), snapshots of droplets at $t = 1.0$ ns (middle panel), and the carbon atoms in contact with the droplet (bottom panel, highlighted by white color) on the 3 × 3 base nanopillars and in the Cassie state. The measured contact angle and the number of water molecules are (a) (134°, 8412) (left column), (b) (143°, 24 204) (middle column), and (c) (140°, 26 532) (right column).

Figure 2, we assume that the true value of the maximum is between values of the last circle and the first cross on the same curve and that the error bar is less than one-half of the difference between the two values. With both assumptions, the error bar of the maximum number of water molecules is estimated to be less than 10%. On the other hand, when the size of the droplet is less than the lower-size limit plotted in Figure 2, we find that the state of the water droplet changes from the Cassie state to the Wenzel state because the droplet size is too small to stay in the Cassie state.

Figure 4 shows the initial configuration of the droplets and snapshots of droplets at 1.0 ns when the droplets are initially in the Wenzel state. Again, the contact angle increases with increasing the size of the droplet. The difference in the recorded contact angle between this case (Wenzel initial state) and the previous one (Cassie initial state) is about 4°. The maximum number of water molecules that can be supported by the 2 × 2 base nanopillars is about N = 5182 (Figure 4b). Under the initial condition of Figure 4c (top panel), the droplet starts to make contact with more nanopillars beyond the initially assigned base nanopillars. As such, the number of base nanopillars changes from 2 × 2 to 2 × 3 in the final state (t = 1.0 ns), as shown in SI Movie S2 . The maximum size is less than that under the initial condition of being in the Cassie state. The reason is possibly because water molecules can be present between the base nanopillars when the droplet is in the Wenzel state. Thus, the center of mass of the droplet is closer to the substrate. As such, water molecules in the lower half of the droplet tend to be driven further from the initially assigned nanopillars. Therefore, the probability of the droplets being in contact with more nanopillars is higher than that when the droplet is initially in the Cassie state. Note that if the size of the droplets is less than the lower size limit as shown in Figure 2, the droplets are always in the Wenzel state. In this case, the contact angle is difficult to estimate due to large fluctuation in the shape of the droplets. So the minimum droplet size that the 2 × 2 base nanopillars can support is not given here.

Next, we consider droplets initially in contact with the larger 3 × 3 base nanopillars and in the Cassie state. Snapshots of water droplets at 1.0 ns are shown in Figure 5. For the smallest droplet, the brightness of the corner nanopillars among the 3 × 3 base nanopillars is weaker than that of other nanopillars (Figure 5a). This indicates that the droplet periodically attaches to or detaches from the corner nanopillars as shown in SI Movie S3 . The size of the droplet in this case is close to the minimum size. If the droplet is less than the minimum size, the number of base nanopillars in contact with water would decrease to 3 × 2 or 2 × 2. Recall that in Figure 2 we show the contact angle increases with increasing the size of droplets, and it reaches the maximum at N = 24 204 (Figure 5b). In that case, the size of the maximum droplet is close to the minimum size in this case. On the other hand, if the droplet size is larger than the maximum size in this case, the number of base nanopillars in contact with the droplet would become larger than 3 × 3, and the contact angle would then start to decrease (see Figure 5c and SI Movie S4).

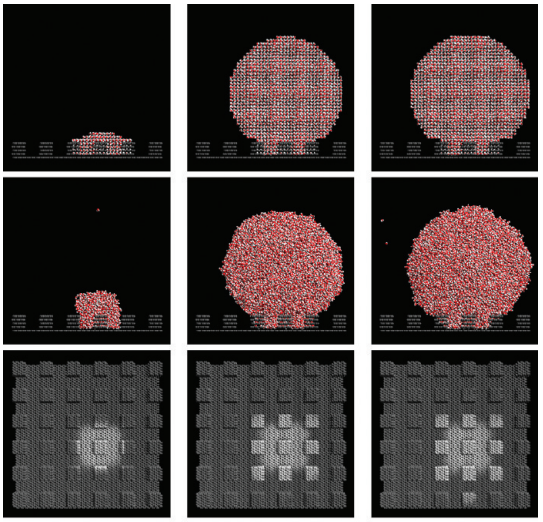

Figure 6. Initial configurations (top panel), snapshots of droplets at $t = 1.0$ ns (middle panel), and the carbon atoms in contact with the droplet (bottom panel, highlighted by white color) on the 3 × 3 base nanopillars and in the Wenzel state. The measured contact angle and the number of water molecules are (a) (91°, 1228) (left column), (b) (141°, 22 220) (middle column), and (c) (140°, 24 476) (right column).

For the droplets being initially in the Wenzel state, snapshots of water droplets at 1.0 ns are shown in Figure 6. For the smallest droplet (Figure 6a), it is pinned by the inner faces of four nanopillars next to the center pillar (all belong to the base nanopillars). Since the fluctuation of the contact angle is large, the contact angle of the droplet is not presented here. The maximum size of a droplet that can be supported by the 3 × 3 base nanopillars is about $N = 22\,220$ (Figure 6b) when the droplet is initially in the Wenzel state, corresponding to the peak shown in Figure 2. If the droplet is larger than the maximum size, the droplet would start to be in contact with more nanopillars beyond the initially assigned 3 × 3 base nanopillars, thereby reducing the contact angle (see Figure 6c and SI Movie S5). The difference between the contact angle in the Cassie and in the Wenzel state decreases with increasing the size of droplets, ranging from about 6° to 1°.

Figure 7 shows the contact angle of a droplet in contact with 4 × 4 base nanopillars in the Cassie state and Wenzel state. The difference in the contact angle between the Cassie and Wenzel states is about 6°. The crosses in Figure 7 also refer to the size of the droplet, which becomes too small or too large to be supported by the original base nanopillars in the same manner as in Figure 2. The triangles correspond to the contact angle of a droplet in which the base nanopillars are 4 × 4 without the corner nanopillars. We discuss this behavior below.

Lastly, we consider the largest 4 × 4 base nanopillars initially assigned to be in contact with droplets. Snapshots of water droplets are shown in Figure 8. The

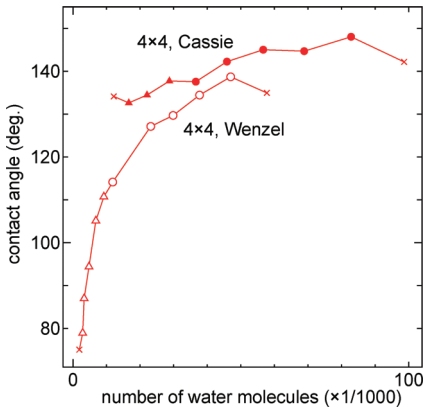

Figure 7. Droplet size dependence of contact angle for a droplet in contact with 4 × 4 base nanopillars, in the Cassie state (filled circles and triangles) and in the Wenzel state (open circles and triangles). The triangles refer to the contact angle for the droplet in contact with 4 × 4 − 4 base nanopillars (see the text).

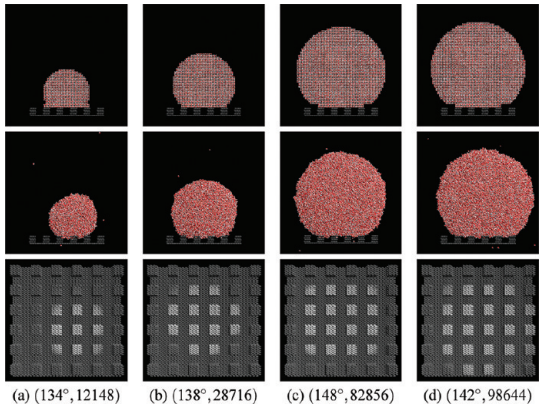

Figure 8. Initial configurations (top panel), snapshots of droplets at $t = 1.0$ ns (middle panel), and the carbon atoms in contact with the droplet (bottom panel, highlighted by white color) on the 4 × 4 base nanopillars and in the Cassie state. The measured contact angle and the number of water molecules are (a) (134°, 12 148), (b) (138°, 28 716), (c) (148°, 82 856), and (c) (142°, 98 644) .

droplets are initially in the Cassie state. We find that the maximum size of a droplet that can be supported by the 4 × 4 base nanopillars is $N = 82\,856$ (Figure 8c), and for this size, the contact angle is 148°. When the size of a droplet is greater than the maximum size, the droplet will make contact with additional nanopillars beyond the initial base nanopillars and the contact angle starts to decrease (see Figure 8d and SI Movie S6). In the lower size limit region ($N = 16\,620$–$28\,716$), the droplets are still in contact with 4 × 4 base nanopillars, but excluding the four corner nanopillars (see Figure 8b and SI Movie S7). (Hereafter this nanopillar configuration will be referred to 4 × 4 − 4.) The calculated contact angles in this region are marked by triangles in Figure 7. When the size of a droplet is further reduced, the number of base nanopillars in contact with water decreases to 3 × 3 (see Figure 8a and SI Movie S8), while the contact angle increases. Including the calculated

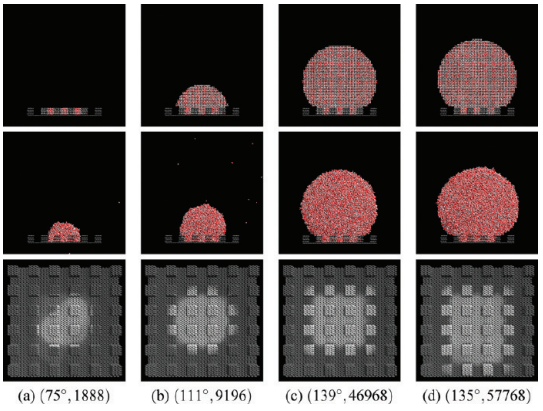

Figure 9. Initial configurations (top panel), snapshots of droplets at $t = 1.0$ ns (middle panel), and the carbon atoms in contact with the droplet (bottom panel, highlighted by white color) on the 4 × 4 base nanopillars and in the Wenzel state. The measured contact angle and the number of water molecules are (a) (75°, 1888), (b) (111°, 9196), (c) (139°, 46 968), and (d) (135°, 57 768).

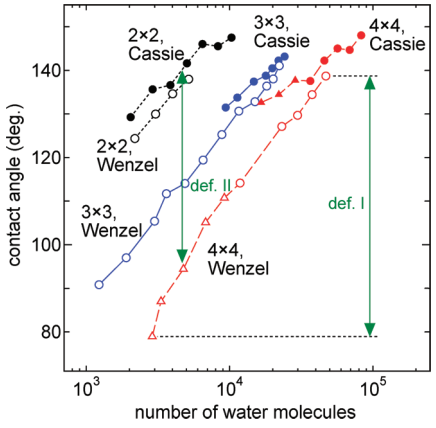

Figure 10. Droplet size dependence of the contact angles based on all data collected from Figure 2 and Figure 7. The *x*-axis is in logarithmic scale. The contact-angle hysteresis based on definition I can be simply calculated as the difference between the angles corresponding to the two end points on any single data line. An example is marked by a green bar (right), for the droplet being placed on the 4 × 4 base nanopillars and in the Wenzel initial state. The contact-angle hysteresis is about 60° (see Table 1). The contact-angle hysteresis based on definition II can be simply calculated by first drawing a vertical line connecting any two data lines and then recording the difference in contact angles corresponding to the two cross points. Each cross point between the vertical line and a data line refers to a different initial state (Cassie or Wenzel, and the number of base nanopillars in contact with the droplet). An example is marked by a green bar (left) between 2 × 2 and 4 × 4 Wenzel states, which gives rise to the contact-angle hysteresis of 42°. Note that definition II can be extended to estimate hysteresis between the Cassie and Wenzel state. An example is the green bar (left) between the 2 × 2 Cassie state and 4 × 4 Wenzel state; that is, one of initial states of the droplet is in the Cassie state and another in the Wenzel state.

contact angles for droplets in contact with 4 × 4 − 4 nanopillars in Figure 8, the minimum size of a droplet is $N = 16\,620$ and the corresponding contact angle is 133°. Therefore, the contact-angle hysteresis is 15° in this case.

When the droplets are initially in the Wenzel state, the maximum size of a droplet that can be supported by the 4 × 4 base nanopillars is $N = 46\,968$ (Figure 9c) and the corresponding contact angle is 139°. If the droplet is larger than the maximum droplet, the contact angle is less than that of the maximum droplet as shown in Figure 9d and SI Movie S9. For droplets in the size range $N = 2888$−9196, the number of base nanopillars in contact with the droplets is 4 × 4 − 4, as shown by triangles in Figure 7. A snapshot at 1.0 ns and the corresponding trajectory are shown in Figure 9b and SI Movie S10, respectively. The contact area for the droplet with size $N = 1888$ cannot fully cover the inner area of the 4 × 4 base nanopillars as shown in Figure 9a and SI Movie S11. Thus, the minimum droplet size is $N = 2888$ and the corresponding contact angle is 79°. Thus, the contact angle hysteresis is 56° when droplets are initially in the Wenzel state and in contact with 4 × 4 base nanopillars. This hysteresis is greater than that when the droplets are initially in the Cassie state.

TABLE 1. Computed Receding and Advancing Angles for the Droplets on 2 × 2, 3 × 3, or 4 × 4 Base Nanopillars and Either in the Cassie or Wenzel State[a]

condition	receding angle	advancing angle	hysteresis
2 × 2, Cassie	(<129°)	148°	(>19°)
2 × 2, Wenzel	(<124°)	138°	(>14°)
3 × 3, Cassie	131°	143°	12°
3 × 3, Wenzel	(<91°)	141°	(>51°)
4 × 4, Cassie	133°	148°	15°
4 × 4, Wenzel	79°	139°	60°

[a] The values in parentheses are lower-size-limit contact angle values shown in Figure 2 (see the text).

DISCUSSION

Figure 10 summarizes calculated contact angle *versus* droplet size. Also, in Table 1, we list all the calculated advancing angles. Note that due to the large fluctuation of droplets, the receding angles cannot be accurately determined except for droplets on 3 × 3 and 4 × 4 base nanopillars and in the Cassie state and on 4 × 4 base nanopillars and in the Wenzel state. For other cases, we use the angles that correspond to the lower size limit angles shown in Figure 10 to estimate the contact-angle hysteresis (definition I), as shown in Table 1. For the larger droplets, it is clear that the contact-angle hysteresis in the Cassie state is less than that in the Wenzel state. The difference in the advancing angle between the Cassie and Wenzel state is very small. On the other hand, the difference in the receding angle is quite large. Especially, in the Wenzel state, the droplets can be in contact with the inner faces of the outer nanopillars, as shown Figure 6a. Hence, the minimum contact angle in the Wenzel state is much smaller than that in the Cassie state.

We note that in the conventional definition of contact-angle hysteresis, the hysteresis is associated with

advancing/receding of the contact line. In experimental measurements, the contact area between the droplet and the substrate is fixed, while the size (or volume) of the droplet is varied by control. Hence, the conventional definition describes the hysteresis for droplets being either in the Wenzel state or in the Cassie state. The Cassie–Wenzel transition is not addressed in the conventional definition. On the other hand, one may ask the question of how the physics behind the contact-angle hysteresis manifests if the size (or volume) of the droplet is fixed while the contact area between the droplet and the substrate is be varied through controlling the shape of the droplet. Can the effect of the Cassie–Wenzel transition be included as part of contact-angle hysteresis? Answers to the two questions lead to a test of a different definition of the contact-angle hysteresis. Unlike the conventional definition that the hysteresis is associated with advancing/receding of the contact line, in the second definition, the hysteresis is associated with different energy states of the droplet when it is in contact with different areas of the substrate. The idea is motivated from the appearance of the so-called hysteresis loop typically seen in computer simulation of the first-order phase transition, where the loop stems from metastability of the system in different thermodynamic states. Since the initial shape of the droplet can be controlled quite arbitrarily in the computer simulation, the number of base nanopillars that are in contact with the droplet can be controlled as well. As an illustration of metastability of the droplet in contact with a different number of base nanopillars, in Table 2, we list the potential energies, E_{pot}, due to water–water and water–graphite (substrate) contribution for a droplet on 2 × 2, 3 × 3, or 4 × 4 base nanopillars and in the Wenzel state. The number of water molecules in the droplet was about 5000. The difference in the potential energy reflects that the droplet is in a different energy state, due in part to a different contact area between the droplet and base nanopillars. The droplet on the 2 × 2 base nanopillars has a nearly spherical shape (Figure S1), and in this case, the water–water potential energy is expected to be the lowest. As the size of droplet increases, it is expected that the energy differences among metastable states of the droplet become smaller so that the droplet could transform spontaneously from the Cassie to the Wenzel state.

The new definition is particularly suited for computer simulation because the initial shape of the droplet and the contact area between the droplet and substrate can be conveniently controlled by design (in experiments, the initial shape of the droplet can be controlled to a certain extent, *e.g.*, by either placing the droplet very gently on a surface or by dropping the droplet from different heights[5]). It offers an alternative way to characterize the magnitude of the contact-angle hysteresis on a rough surface. Specifically, the contact-angle hysteresis based on the second definition can be estimated

TABLE 2. Potential Energy, E_{pot}, of Water–Water and Water–Graphite Contribution at 2 × 2, 3 × 3, and 4 × 4 Base Nanopillars Either in the Cassie or Wenzel State[a]

condition	number of molecules	E_{pot} (kcal/mol)	ΔE_{pot}[b] (kcal/mol)
2 × 2, Wenzel	4890	−8.55	
3 × 3, Wenzel	4885	−8.32	0.23
4 × 4, Wenzel	4764	−2.54	6.01
2 × 2, Cassie	4864	−7.31	1.23

[a] The numbers of molecules are almost the same and correspond to the position under the vertical arrow of definition II in Figure 10. [b] The difference of the potential energy from E_{pot} of 2 × 2, Wenzel.

by using the contact angles collected in Figure 10. In the Cassie state, the droplets can be placed on the 2 × 2 or 3 × 3 base nanopillars, with the size of droplets ranging from 8400 to 10 000, or on the 3 × 3 or 4 × 4 − 4 base nanopillars with the number of water molecules ranging from 16 000 to 24 000. In the Wenzel state, the droplets can be placed on the 2 × 2, 3 × 3, or 4 × 4 base nanopillars, with the number of water molecules ranging from 3000 to 5000, or on the 3 × 3 or 4 × 4 base nanopillars with the number of water molecules ranging from 3000 to 23 000. In these size ranges of water molecules, there are many variances for the contact area between the droplet and the base nanopillars, depending on the initial shape of the droplets. The difference in the contact angle between the cases of 2 × 2 and 3 × 3 base nanopillars amounts to about 13° in the Cassie state and 23° in the Wenzel state. The difference in the calculated contact angle between the cases with 3 × 3 and 4 × 4 base nanopillars amounts to about 7° in the Cassie state and 18° in the Wenzel state. In addition, the difference in the contact angle between the cases with 2 × 2 and 4 × 4 base nanopillars amounts to about 46° when the droplets are in the Wenzel state. These differences can be used to quantify contact-angle hysteresis based on definition II. Moreover, definition II can be extended to estimate hysteresis between the Cassie and Wenzel state (see Figure 10).

Again, we find that the contact-angle hysteresis in the Cassie state is weaker than that in the Wenzel state, regardless of the definition. If a droplet size is much larger than the microscopic roughness of the surface, the contact area between the droplet and the rough surface could be changed continuously. More importantly, the contact angle would be independent of the size of droplets in the large-size limit. Hence, the contact-angle hystereses calculated based on definitions I and II are expected to be consistent with each other in this limit.

Note that the Wenzel formula[2] is given by

$$\cos \theta_w = r \cos \theta \quad (1)$$

where θ_w is the contact angle in the Wenzel state on the rough surface, r is the ratio of the actual area of the rough surface to the projected area, and θ is the equilibrium contact angle on a flat surface. The Cassie

formula[3] is given by

$$\cos\theta_c = \phi_s(\cos\theta + 1) - 1 \quad (2)$$

where θ_c is the contact angle on the composite surface and ϕ_s is the area fraction of the solid surface. Using the Cassie and Wenzel formulas, the calculated contact angles are 139° and 94°, respectively. Here, 92° is used for the contact angle on a flat surface, which is taken from our previous paper.[15] The value 139° is very close to the contact angle value corresponding to the mid-point of the three Cassie curves (solid points) in Figure 10. The value 94° is fairly close to the minimum value of the contact angle for a droplet on the 3 × 3 base nanopillars and in the Wenzel state (see Figure 10). Although the Cassie formula does not take into account size and pinning effects, the calculated contact angle seems quite close to the mid-point value of the contact angle curve measured from the MD simulations.

CONCLUSION

We have performed MD simulations to study the contact-angle hysteresis of water droplets on a nanopillared surface and in two possible states (Cassie and Wenzel). The number of water molecules in the droplets is varied by design to simulate addition or removal of volumes of droplets as done in the experiments. We consider three initial contact areas (on a rough substrate) for the droplets: the 2 × 2, 3 × 3, and 4 × 4 base nanopillars. The Cassie and Wenzel states are assigned as two possible initial states for the droplets. From MD simulations, we can measure the contact-angle hysteresis by using either the conventional approach (based on definition I) or a new approach (based on definition II). In definition I, the contact-angle hysteresis refers to the difference in the measured contact angle for the droplet in direct contact with the same base nanopillars but with gradually changed volumes, while in definition II, the contact-angle hysteresis refers to the difference in the measured contact angle for the droplet with the same volume but having different initial contact area with the substrate. According to definition I, the contact angles of droplets with the minimum or the maximum volumes are designated as the receding and advancing contact angle, respectively. We have measured the advancing contact angles for all initial conditions. The receding contact angles are measured only under the initial contact with 3 × 3 base nanopillars in the Cassie state and with 4 × 4 base nanopillars in the Cassie and Wenzel states. Although only nanoscale droplets are involved in our simulation, the contact-angle hysteresis in the Cassie state is evidently smaller than that in the Wenzel state. This conclusion seems universal and is consistent with the experimental measurement.[6] Alternatively, we find that droplets with the same volume can reach different metastable states on either the 2 × 2, 3 × 3, or 4 × 4 base nanopillars within a certain range of droplet sizes. This phenomenon leads to definition II of contact-angle hysteresis. We note that definition II can be extended to estimate hysteresis between the Cassie and Wenzel state. Again, with the new definition, we find that the contact-angle hysteresis in the Cassie state is still weaker than that in the Wenzel state.

SIMULATION METHOD

Our MD simulations are carried out in the constant-volume and constant-temperature (298 K) ensemble. The temperature is controlled by using the velocity scaling method. The periodic boundary condition is applied in all three spatial dimensions. A rigid-body model of water, *i.e.*, the SPC/E model,[23] is employed. The potential function of the SPC/E model includes two terms, a Coulomb term and a Lennard-Jones (LJ) term. The long-range charge−charge interaction between water molecules is calculated by using the Ewald method. Carbon atoms of the graphite are treated as LJ particles whose size and energy parameters are 3.4 Å and 0.2325 kJ/mol, respectively.[24] The time integration of the translational and rotational motion is undertaken using the velocity Verlet method and time-reversible algorithm.[25] The MD time step is set at 2.0 fs. Each MD simulation is 1.0 ns.

In the initial configuration, the contact area of a droplet is predetermined; that is, the droplet is in contact with a known number of base nanopillars. The initial coordination of water molecules is set as that of a simple cubic lattice with the same density as bulk water. The initial droplet can be in either the Wenzel or Cassie state. The number of water molecules, N, ranges from 2000 to 100 000. In the beginning of MD simulations, translational motion of water molecules is not involved for 2.0 ps so that only orientational degrees of freedom of water molecules are relaxed.

To measure the contact angle, we use the following computational approach to map out the surface locus of a water nanodroplet. We divide the entire simulation cell into many cubic meshes, each with length scale of 5 Å. The average local water density in each cubic mesh is recorded. With the obtained local water density, we can identify the spatial points where the local density is half of the bulk water density. The locus of these points represents the surface of the droplet. The contact angle is defined as the angle between a tangential line of the droplet surface (described by a fitting curve) through any three-phase contact point and another line within the flat surface (through the top of the nanopillars) and through the same three-phase contact point. Both lines must be in the plane through the center of the droplet. We use the late 500 ps of MD runs to compute the contact angles. The computed contact angle for a water droplet on a graphite surface is 92°.[15]

Because the system size involved in the simulation is fairly large, a special-purpose computer, "MDGRAPE-3",[26−28] is used to perform the MD simulations. The peak performance of a MDGRAPE-3 board at 250 MHz is 2.16 TFLOPS. We have utilized two special-purpose computers for the MD simulation: one for the real part of the Ewald calculation and the other for the reciprocal-space part of the Ewald calculation.

Finally, we note that all simulations presented above are based on the system with identical nanopillars whose cross-section is square-shaped. We have also examined a system with

identical cylinder nanopillars but with a smaller cross-section area than the square-shaped nanopillars. An independent simulation is performed with droplets initially placed on the 3×3 base nanopillars and in either the Wenzel or Cassie initial state. We find that the size and shape of the nanopillar cross-section can affect the final state of the droplet, especially in the Cassie state (see Figure S2).

Acknowledgment. This work was supported by the Asahi Glass Foundation. X.C.Z. is supported by U.S. NSF (grant nos. EPS-1010674 and CBET-1066947) and ARL (grant no. W911-NF1020099).

Supporting Information Available: Movies of droplets on a nanopillared surface, movies of highlighted carbon atoms that are in direct contact with the droplets, and a plot of contact angle *versus* the number of water molecules are collected. This material is available free of charge *via* the Internet at http://pubs.acs.org.

REFERENCES AND NOTES

1. Johnson, R. E.; Dettre, R. H. Contact Angle, Wettability, and Adhesion. *Adv. Chem. Ser.* **1964**, *43*, 112–144.
2. Wenzel, R. N. Resistance of Solid Surfaces to Wetting by Water. *Ind. Eng. Chem.* **1936**, *28*, 988–994.
3. Cassie, A. B. D.; Baxter, S. Wettability of Porous Surfaces. *Trans. Faraday Soc.* **1944**, *40*, 546–551.
4. Patankar, N. A. On the Modeling of Hydrophobic Contact Angles on Rough Surfaces. *Langmuir* **2003**, *19*, 1249–1253.
5. He, B.; Patankar, N. A.; Lee, J. Multiple Equilibrium Droplet Shapes and Design Criterion for Rough Hydrophobic Surfaces. *Langmuir* **2003**, *19*, 4999–5003.
6. Lafuma, A.; Quéré, D. Superhydrophobic States. *Nat. Mater.* **2003**, *2*, 457–460.
7. Reyssat, M.; Quéré, D. Contact Angle Hysteresis Generated by Strong Dilute Defects. *J. Phys. Chem. B* **2009**, *113*, 3906–3909.
8. Extrand, C. W. Model for Contact Angles and Hysteresis on Rough and Ultraphobic Surfaces. *Langmuir* **2002**, *18*, 7991–7999.
9. Liu, Y.; Chen, X.; Xin, J. H. Can Superhydrophobic Surfaces Repel Hot Water? *J Mater. Chem.* **2009**, *19*, 5602–5611.
10. Kong, B.; Yang, X. Dissipative Particle Dynamics Simulation of Contact Angle Hysteresis on a Patterned Solid/Air Composite Surface. *Langmuir* **2006**, *22*, 2065–2073.
11. Dorrer, C.; Ruhe, J. Contact Line Shape on Ultrahydrophobic Post Surfaces. *Langmuir* **2007**, *23*, 3179–3183.
12. Kusumaatmaja, H.; Yeomans, J. M. Modeling Contact Angle Hysteresis on Chemically Patterned and Superhydrophobic Surfaces. *Langmuir* **2007**, *23*, 6019–6032.
13. Hong, S. D.; Ha, M. Y.; Balachandar, S. Static and Dynamic Contact Angles of Water Droplet on a Solid Surface Using Molecular Dynamics Simulation. *J. Colloid Interface Sci.* **2009**, *339*, 187–195.
14. Dupont, J.-B.; Legendre, D. Numerical Simulation of Static and Sliding Drop with Contact Angle Hysteresis. *J. Comput. Phys.* **2010**, *229*, 2453–2478.
15. Koishi, T.; Yasuoka, K.; Fujikawa, S.; Ebisuzaki, T.; Zeng, X. C. Coexistence and Transition between Cassie and Wenzel State on Pillared Hydrophobic Surface. *Proc. Natl. Acad. Sci. U. S. A.* **2009**, *106*, 8435–8440.
16. Koishi, T.; Yasuoka, K.; Zeng, X. C.; Fujikawa, S. Molecular Dynamics Simulations of Urea−Water Binary Droplets on Flat and Pillared Hydrophobic Surfaces. *Faraday Discuss.* **2010**, *146*, 185–193.
17. Hirvi, J. T.; Pakkanena, T. A. Molecular Dynamics Simulations of Water Droplets on Polymer Surfaces. *J. Chem. Phys.* **2006**, *125*, 144712 1–11.
18. Ingebrigtsen, T.; Toxvaerd, S. Contact Angles of Lennard-Jones Liquids and Droplets on Planar Surfaces. *J. Phys. Chem. C* **2007**, *111*, 8518–8523.
19. Herring, A. R.; Henderson, J. R. Simulation Study of the Disjoining Pressure Profile through a Three-Phase Contact Line. *J. Chem. Phys.* **2010**, *132*, 084702 1–12.
20. Dimitrov, D. I.; Milchev, A.; Binder, K. Method for Wettability Characterization Based on Contact Line Pinning. *Phys. Rev. E* **2010**, *81*, 041603.
21. Lundgren, M.; Allan, N. L.; Cosgrove, T.; George, N. Wetting of Water and Water/Ethanol Droplets on a Non-Polar Surface: A Molecular Dynamics Study. *Langmuir* **2002**, *18*, 10462–10466.
22. Lundgren, M.; Allan, N. L.; Cosgrove, T.; George, N. Molecular Dynamics Study of Wetting of a Pillar Surface. *Langmuir* **2003**, *19*, 7127–7129.
23. Beredensen, H. J. C.; Grigera, J. R.; Straatsma, T. P. The Missing Term in Effective Pair Potentials. *J. Phys. Chem.* **1987**, *91*, 6269–6271.
24. Bhethanabotla, V. R.; Steele, W. A. Molecular Dynamics Simulations of Oxygen Monolayers on Graphite. *Langmuir* **1987**, *3*, 581–587.
25. Matubayasi, N.; Nakahara, M. Reversible Molecular Dynamics for Rigid Bodies and Hybrid Monte Carlo. *J. Chem. Phys.* **1999**, *110*, 3291–3301.
26. Taiji, M.; Narumi, T.; Ohno, Y.; Futatsugi, N.; Suenaga, A.; Takada, N.; Konagaya, A. Protein Explorer: A Peta Flops Special-Purpose Computer System for Molecular Dynamics Simulations. *Proceedings of the SC2003 (High Performance Networking and Computing)*, Phoenix, AZ, USA, Nov 15−21, 2003. http://www.supercomp.org/sc2003/archive/sc2003/paperpdfs/pap168.pdf (accessed Aug 2, 2011).
27. Taiji, M. MDGRAPE-3 chip: A 165-Gflops Application-Specific LSI for Molecular Dynamics Simulations. *Proceedings of the HOT CHIPS 16 (A Symposium on High Performance Chips)*, Stanford, CA, USA, Aug 22−24, 2004. http://www.hotchips.org/archives/hc16 (accessed Aug 2, 2011).
28. Narumi, T.; Ohno, Y.; Okimoto, N.; Koishi, T.; Suenaga, A.; Futatsugi, N.; Yanai, R.; Himeno, R.; Fujikawa, S.; Ikei, M.*et al.* A 55 TFLOPS Simulation of Amyloid-Forming Peptides from Yeast Prion Sup35 with the Special-Purpose Computer System MDGRAPE-3. *Proceedings of the SC06 (High Performance Computing, Networking, Storage and Analysis)*, Tampa, FL, USA, Nov 11−17, 2006. http://sc06.supercomputing.org/schedule/pdf/gb106.pdf (accessed Aug 2, 2011).